JOURNAL OF THE AMERICAN CHEMICAL SOCIETY

Subscriber access provided by Olson Library | Northern Michigan University

Article

Mechanism of Molybdenum Mediated Carbon Monoxide Deoxygenation and Coupling: Mono- and Dicarbyne Complexes Precede C–O Bond Cleavage and C–C Bond Formation

Joshua A. Buss, and Theodor Agapie

J. Am. Chem. Soc., **Just Accepted Manuscript** • DOI: 10.1021/jacs.6b10535 • Publication Date (Web): 21 Nov 2016

Downloaded from http://pubs.acs.org on November 21, 2016

Just Accepted

“Just Accepted” manuscripts have been peer-reviewed and accepted for publication. They are posted online prior to technical editing, formatting for publication and author proofing. The American Chemical Society provides “Just Accepted” as a free service to the research community to expedite the dissemination of scientific material as soon as possible after acceptance. “Just Accepted” manuscripts appear in full in PDF format accompanied by an HTML abstract. “Just Accepted” manuscripts have been fully peer reviewed, but should not be considered the official version of record. They are accessible to all readers and citable by the Digital Object Identifier (DOI®). “Just Accepted” is an optional service offered to authors. Therefore, the “Just Accepted” Web site may not include all articles that will be published in the journal. After a manuscript is technically edited and formatted, it will be removed from the “Just Accepted” Web site and published as an ASAP article. Note that technical editing may introduce minor changes to the manuscript text and/or graphics which could affect content, and all legal disclaimers and ethical guidelines that apply to the journal pertain. ACS cannot be held responsible for errors or consequences arising from the use of information contained in these “Just Accepted” manuscripts.

ACS Publications

Journal of the American Chemical Society is published by the American Chemical Society. 1155 Sixteenth Street N.W., Washington, DC 20036

Published by American Chemical Society. Copyright © American Chemical Society. However, no copyright claim is made to original U.S. Government works, or works produced by employees of any Commonwealth realm Crown government in the course of their duties.

Mechanism of Molybdenum Mediated Carbon Monoxide Deoxygenation and Coupling: Mono- and Dicarbyne Complexes Precede C–O Bond Cleavage and C–C Bond Formation

Joshua A. Buss and Theodor Agapie*

Division of Chemistry and Chemical Engineering, California Institute of Technology, 1200 E. California Blvd. MC 127-72, Pasadena, CA, USA

ABSTRACT: Deoxygenative coupling of CO to value-added $C_{\geq 2}$ products is challenging and mechanistically poorly understood. Herein we report a mechanistic investigation into the reductive coupling of CO, which provides new fundamental insights into a multi-electron bond breaking and bond making transformation. In our studies, the formation of a bis(siloxycarbyne) complex precedes C–O bond cleavage. At -78 °C, over days, C–C coupling occurs without C–O cleavage. However, upon warming to 0 °C, C–O cleavage is observed from this bis(siloxycarbyne) complex. A siloxycarbyne/CO species undergoes C–O bond cleavage at lower temperatures, indicating that monosilylation, and a more electron rich Mo center, favors deoxygenative pathways. From the bis(siloxycarbyne), isotopic labeling experiments and kinetics are consistent with a mechanism involving unimolecular silyl loss or C–O cleavage as rate determining steps toward carbide formation. Reduction of Mo(IV) CO adducts of carbide and silylcarbyne species allowed for the spectroscopic detection of reduced silylcarbyne/CO and mixed silylcarbyne/siloxycarbyne complexes, respectively. Upon warming, both of these silylcarbynes undergo C–C bond formation, releasing silylated C_2O_1 fragments and demonstrating that the multiple bonded terminal Mo≡C moiety is an intermediate on the path to deoxygenated, C–C coupled products. The electronic structures of Mo carbide and carbyne species were investigated quantum mechanically. Overall, the present studies establish the elementary reactions steps by which CO is cleaved and coupled at a single metal site.

1. INTRODUCTION

With the rise of atmospheric carbon dioxide (CO_2) levels and geopolitical constraints on the availability of reduced carbon reserves, there is significant interest in the generation of liquid fuels from oxygenated C_1 feedstocks.[1,2] Synthesis gas (syngas), a mixture of carbon monoxide (CO) and dihydrogen (H_2), is one such feedstock obtained from biomass, coal, and natural gas.[3,4] Using syngas as an alternative to crude petroleum for the generation of fuels and chemical precursors is demonstrated in the Fischer-Tropsch (F–T) process; F–T converts syngas to a complex mixture of hydrocarbons at high temperatures on heterogeneous surfaces.[3-5] Increasing the selectivity of F–T is of significant interest and a recent report demonstrates that decoupling CO activation and C–C bond formation is a viable strategy.[6] Deeper mechanistic insight into the elementary transformations involved in F–T holds promise for developing more efficient and selective catalysts. However, detection of reaction intermediates in these systems is challenging.[3-5]

Molecular systems have been studied extensively to gain insight into the steps of reductive CO coupling chemistry.[3] Leveraging strong M–O interactions,[7-17] insertion into early transition-metal hydride bonds,[18-25] inducing radical character at carbon,[26,27] and electrophilic functionalization[28-33] have all proven viable strategies for CO reduction, C–O bond cleavage, and C–C bond formation. The addition of silyl electrophiles to electron-rich dicarbonyl complexes forms bound bis(siloxy)acetylene units,[28-30,32,34] a two-electron reduced CO coupling product. This reaction proceeds through a silylated dicarbyne complex,[33,34] and, following hydrogenation, can yield metal-free siloxy-substituted olefins.[32-34] Although these alkenes represent a four-electron reduced CO-derived product, both C–O bonds of the starting COs remain intact. It is rare that both C–O bond cleavage and C–C bond formation are simultaneously achieved in homogeneous model systems.[15,24,25]

This is in stark contrast to the product distributions found for CO coupling catalysis in F–T,[4,5] by oxide-derived Cu electrodes,[35] and by nitrogenase enzymes.[36,37] The hydrocarbons and alcohols formed in these systems require at least one C–O bond breaking step. Despite experimental[38-40] and computational[41,42] studies, insight into the operative mechanisms of the electrocatalytic and enzymatic systems is sparse. Most mechanistic proposals for the more thoroughly studied F–T process invoke C–O bond cleavage to a surface carbide prior to C–C coupling.[3] Only a handful of homogeneous complexes bearing bridging[17,43] and terminal[44-46] carbides have been synthesized from CO, overcoming the strong C≡O triple bond (257 kcal/mol).[47] Functionalization of these carbides with electrophiles provides alkylidynes,[44,45] motifs that have been shown to undergo C–C bond formation with CO ligands,[48-52] but only recently has a terminal transition metal carbide been clearly demonstrated as an intermediate in a homogeneous CO coupling reaction.[46]

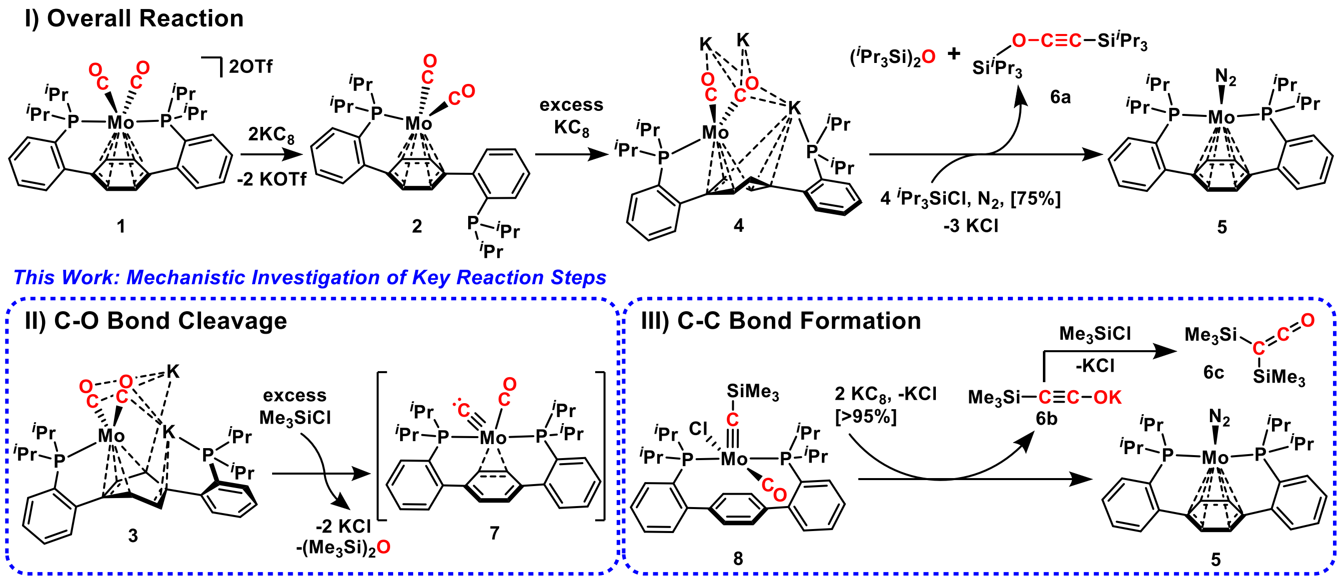

Scheme 1: CO activation, cleavage, and coupling at a single Mo center.[46]

Taking advantage of the coordinative flexibility and redox activity of noninnocent *para*-terphenyldiphosphine ligands,[53-59] we have recently described the role of complexes **1**-**8** in C–O bond cleavage and C–C bond formation between two highly activated CO ligands (Scheme 1). Terminal Mo carbide **7** was proposed as the product of C–O bond cleavage (Scheme 1, II) and Mo silylcarbyne **8** was demonstrated as a precursor to C–C coupling (Scheme 1, III), resulting in a four-electron reduced C_2O_1 fragment (Scheme 1, **6c**). In the present study, we provide a more detailed and complete mechanistic picture of the pivotal C–O bond cleaving and C–C bond forming steps in this complex reaction sequence, including the characterization of several reaction intermediates.

2. RESULTS AND DISCUSSION

2.1. Previously Reported Molybdenum Dicarbonyl Complexes. We recently described the synthesis and characterization of polyanionic dicarbonyl complexes **3** and **4**.[46] A full description of their structural details follows. Dianion **3** crystallizes as a potassium bridged dinuclear cluster—two Mo(CO)$_2$ units are bridged by four potassium ions. The cations display interactions with the carbonyl ligands, the dangling phosphine arm, the central arenes of the terphenyl backbone, and solvating THF molecules. Significant distortion of the central arene from planarity is observed, with an angle of 46.2° between the C_6–C_1–C_2–C_3 and C_6–C_5–C_4–C_3 planes. This deplanarization, as well as localization of short C–C contacts between C_1 and C_2 and C_4 and C_5 (Figure 1), is consistent with partial cyclohexadienyldianionic character.[60,61] Notably, the dianion shows Mo–CO and C–O bond metrics that are significantly contracted and elongated, respectively, from neutral species **2** (Figure 1).

Trianion **4** likewise adopts a polynuclear structure—a Mo_4K_{12} tetramer—in the solid state. Two disparate $K_3Mo(CO)_2$ subunits are observed. One is quite similar in structure to dianion **3**, with an η^4 metal-arene interaction, a deplanarization of the central arene ring of 43.7°, and short Mo–CO and long C–O contacts (Figure 1, **4-η^4**). The second subunit has antifacial phosphines, one coordinating Mo and the other a potassium cation, on opposite faces of the central ring (Figure 1, **4-η^3**).

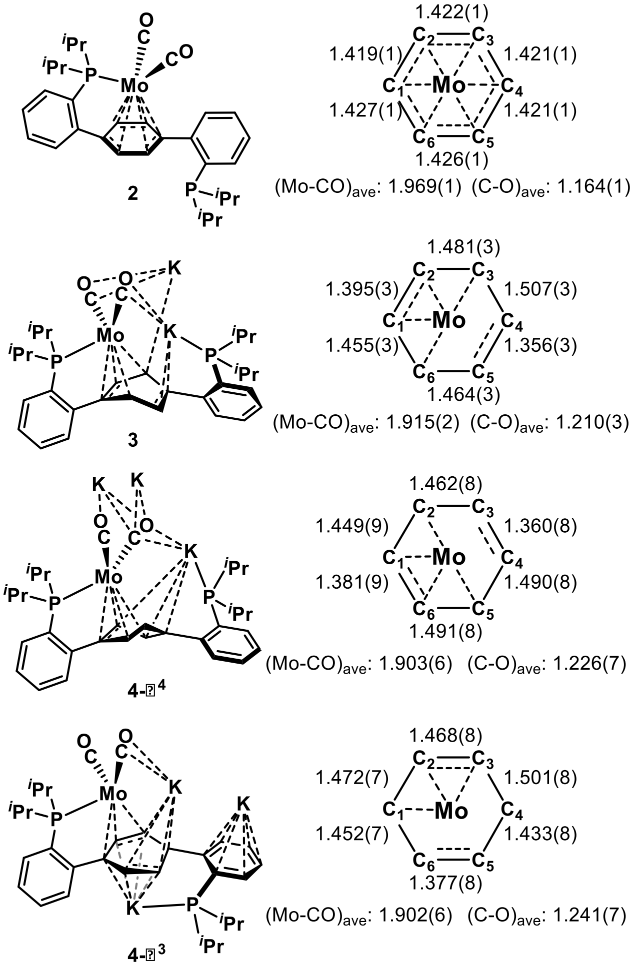

Figure 1: Line representations (left) and bond metrics (right) as determined by single-crystal XRD for dicarbonyl complexes **2**-**4**. For anions **3** and **4**, representative mononuclear $K_nMo(CO)_2$ fragments of the polynuclear complexes are shown. All bond distances are reported in Å.

This arene ring, which displays η^3 Mo-allyl character,[56] has two cation-π interactions with the potassium counter ions[62] and is more planar ($\angle C_3–C_2–C_1)(C_3–C_4–C_6–C_1) = 34.8°$). The Mo–C and C–O distances are comparable in both the η^3 and η^4-bound components, and along with the arene bond metrics, support significant delocalization of the stored reducing equivalents between the central ring, Mo center, and CO ligands. Formal oxidation state assignments of Mo in **3** and **4** are complicated by this high degree of charge delocalization.

2.2. Variable Temperature NMR Studies of Electrophilic Quenching of Anion 3. Variable temperature (VT) NMR studies monitoring addition of both small and large silyl electrophiles to complex **3** were conducted in an attempt to spectroscopically characterize reaction intermediates.

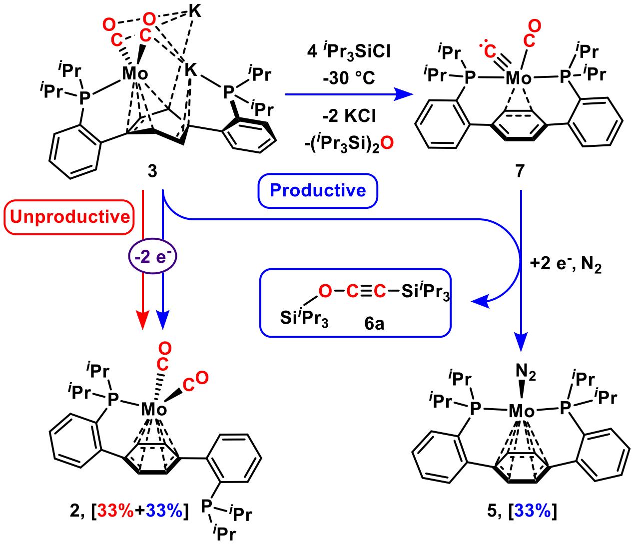

Scheme 2: ^{i}Pr$_3$SiCl addition to dianion **3**. Product distribution, as determined by ^{31}P{^{1}H} NMR spectroscopy, is shown in brackets.

2.2.1. VT NMR Studies of Reaction With ^{i}Pr$_3$SiCl. A solution of ^{13}CO enriched dianion **3** (**3-^{13}C**) was treated with four equiv. of ^{i}Pr$_3$SiCl at -78 °C (Scheme 2). No reaction was observed at this temperature by ^{31}P{^{1}H} or ^{13}C{^{1}H} NMR spectroscopy. Warming the sample to -30 °C resulted in the appearance of carbide **7-^{13}C**, as a minor species, as indicated by the characteristic low-field carbidic resonance at 547.2 ppm in the ^{13}C{^{1}H} NMR spectrum (Figure S1). Concomitant formation of oxyacetylene **6a**, dinitrogen adduct **5**, and dicarbonyl **2-^{13}C** were observed by coupled doublets at 108.3 and 25.2 ppm (^1J(C,C) = 167.7 Hz) in the ^{13}C{^{1}H} NMR spectrum, a ^{31}P{^{1}H} resonance at 76.4 ppm, and by ^{13}C{^{1}H} (229.9 ppm, d, ^2J(P,C) = 11.1 Hz) and ^{31}P{^{1}H} (95.9 ppm, t, ^2J(P,C) = 11.2 Hz) NMR spectroscopy, respectively. Further warming of the solution resulted in complete conversion to the Mo-N$_2$ complex **5**, oxidized dicarbonyl **2-^{13}C**—in a *ca.* 1:2 ratio (by ^{31}P{^{1}H} NMR)—and the C$_2$O$_1$ organic fragment, **6a**. These data support the intermediacy of carbide **7** in the reaction sequence. No other intermediates were detected.

The observed reactivity is consistent with multiple reaction pathways from dianion **3-^{13}C** (Scheme 2). Productive CO reduction chemistry involves carbonyl silylation and C–O bond cleavage, providing carbide **7-^{13}C** and (^{i}Pr$_3$Si)$_2$O. The intermediate Mo(IV) complex **7-^{13}C** is envisioned to react with an equimolar amount of **3-^{13}C**, which serves as a sacrificial two-electron reductant. This two-electron oxidation of **3-^{13}C** leads to Mo(0) dicarbonyl complex **2-^{13}C**. Reduction of **7-^{13}C** by two electrons coupled with silylation forms the C$_2$O$_1$ species, **6a-^{13}C**, and Mo(0)-N$_2$ complex **5**. The four electrons required for the conversion of two molecules of CO to **6a-^{13}C** are provided by two equivalents of dianion **3-^{13}C**, forming equimolar amounts of the Mo(0) complexes **5** and **2-^{13}C** (depicted in blue in Scheme 2).

The product ratio of **2** and **5** suggests additional unproductive redox chemistry from dianion **3-^{13}C**, likely involving reduction of electrophile (depicted in red in Scheme 2). Though the same products are observed when either dianion **3-^{13}C** or trianion **4-^{13}C** is treated with ^{i}Pr$_3$SiCl at low temperature, the latter reacts quantitatively (in reducing equivalents) toward CO deoxygenative coupling chemistry to form the desired products **5** and **6a** (75% conversion, by ^{31}P{^{1}H} NMR).[46] The quantitative reactivity of trianion **4-^{13}C** suggests that fully pre-loading the complex with electrons promotes C–O reduction chemistry and disfavors unproductive outer-sphere redox, an important feature for designing highly selective systems.

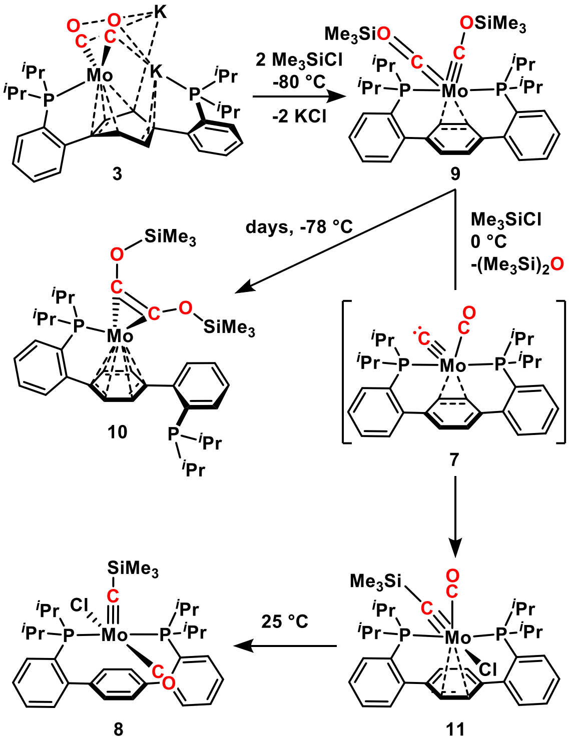

Scheme 3: Me$_3$SiCl mediated C–O cleavage and C–C coupling transformations from dianion **3**.

2.2.2. VT NMR Studies of Reaction With Me$_3$SiCl. The addition of the smaller silyl electrophile, Me$_3$SiCl, to dianion **3-^{13}C** was likewise investigated at low temperature. Thawing a frozen THF solution of **3-^{13}C** and Me$_3$SiCl to -80 °C resulted in the observation of a single triplet resonance at 63.8 ppm (^2J(C,P) = 17.32 Hz) in the ^{31}P{^{1}H} NMR spectrum, indicating that the free phosphine arm in **3-^{13}C** rebinds the Mo center. Two broad resonances at 285.8 and 275.8 ppm were present in the ^{13}C{^{1}H} NMR spectrum (Figure S2). These downfield ^{13}C signals, suggest the formation of dicarbyne **9-^{13}C** (Scheme 3).[63] Similar ^{13}C chemical shifts are reported for siloxycarbyne complexes of Fe (230-260 ppm)[33,64] and Ta

(240 ppm)[65]. To the best of our knowledge, bis(siloxycarbyne) complexes have not been reported for Mo, though analogous bis(aminocarbyne) motifs are known for both Mo and W, with ^{13}C resonances in the range of 250-280 ppm.[66-69]

A *pseudo*-square pyramidal coordination geometry of dicarbyne **9-^{13}C** is proposed with two ^{13}*C*OSiMe$_3$ moieties in distinct chemical environments, axial and equatorial (Figure S2, right), accounting for the two unique resonances observed in the ^{13}C{^{1}H} NMR spectrum at -80 °C. Warming **9-^{13}C** to -20 °C results in coalescence of these resonances to a broad signal at 281.9 ppm, consistent with two Mo≡^{13}*C*OSiMe$_3$ fragments involved in a fast exchange process on the NMR time scale. This fluxionality is attributed to ring-slipping of the η^2-arene interaction on opposite edges of the arene, while also interconverting the axial and equatorial alkylidynes. Cooling the sample to -100 °C returns the disparate signals, and resolves each as a broad triplet (284.9 and 276.0 ppm). These resolved resonances show no ^1J(C,C), demonstrating a lack of a C–C bond and further supporting the dicarbyne assignment. The ^2J(P,C) data from ^{31}P{^{1}H} NMR spectroscopy also support this exchange process (Figure S2).

The spectrum collected at -100 °C, where the carbyne moieties are under the slow exchange limit, was simulated; modeling the exchange dynamics up to -20 °C provided rates for the carbyne exchange (Figure S2). The Eyring equation was used to calculate the activation parameters of this process giving $\Delta G^\ddagger$ = 9.4 ± 0.4 kcal/mol at -40 °C (Table S1), which is in reasonable agreement with the estimated value from the approximate coalescence temperature ($\Delta G^\ddagger$ = 9.9 kcal/mol, T_c = -40 °C). The calculated activation parameters are $\Delta H^\ddagger$ = 6.6 ± 0.4 kcal/mol and $\Delta S^\ddagger$ = -12 ± 2 e.u. (Figure S3). The large and negative $\Delta S^\ddagger$ is consistent with a non-dissociative process with a highly ordered transition state, likely required by the steric constraints of shifting of the two carbyne ligands in the terphenyl diphosphine cleft without phosphine arm dissociation.

Crystallization of bis(siloxycarbyne) **9** was attempted; slow evaporation of liquid butane over days furnished maroon single crystals of a new species corresponding to two electron CO coupling chemistry—bis(siloxy)acetylene complex **10** (Scheme 3). The solid-state structure of **10** (Figure 2) is similar to that of other bis(siloxy)acetylene complexes of group V metals, with a short C$_{31}$–C$_{32}$ distance (1.332(2) Å), an acute C$_{31}$–Mo–C$_{32}$ angle (38.0°), and long C$_{31/32}$–O$_{1/2}$ distances (1.367(2) Å).[30,32] The Mo center adopts an η^6 metal-arene interaction, with coordination of a single phosphine donor.

The ^{31}P{^{1}H} NMR data for the bis(siloxy)acetylene adduct **10-^{13}C** corroborate the conservation of a monophosphine coordination environment in solution, with resonances at 86.7 and -6.8 ppm for the Mo-bound and free phosphines, respectively. The ^{13}C{^{1}H} NMR spectrum shows a single doublet for the acetylene carbons at 207.9 ppm (^2J(C,P) = 19.9 Hz), despite their asymmetry in the solid-state. Holding dicarbyne complex **9-^{13}C** at -78 °C shows slow conversion to C–C coupled **10-^{13}C** by ^{13}C{^{1}H} NMR spectroscopy, providing a route to a metal-bound two-electron reduced CO coupling product (Scheme 3). Importantly, characterization of **10** by crystallography provides indirect structural evidence for proposed dicarbyne **9**, as dicarbyne complexes are demonstrated intermediates in the formation of C$_2$O$_2$ fragments from CO.[28,33,34]

Studies at higher temperatures (-78 °C to room temperature) indicate that acetylene adduct **10** does not undergo C–O bond cleavage chemistry. To mimic reaction conditions in which C–O bond cleavage was observed, **10** was treated with excess Me$_3$SiCl; no reaction was observed. In low temperature reactions of **3** with silyl electrophiles, the dianion itself acts as a reductant (*vide supra*). To probe if **10** reacts under reductive conditions in the presence of Me$_3$SiCl, *in situ* reduction of the above mixture was conducted. Addition of two equiv. of [Na][C$_{10}$H$_8$] at -78 °C resulted in the formation of an intractable mixture as evidenced by ^{13}C{^{1}H} and ^{31}P{^{1}H} NMR (Figure S4). Even upon warming to room temperature, no ^{13}C resonances consistent with C–O cleavage chemistry from **10-^{13}C** were observed, consistent with C–C coupled **10** being off-path to C–O cleavage and the observed four-electron reductive coupling chemistry.

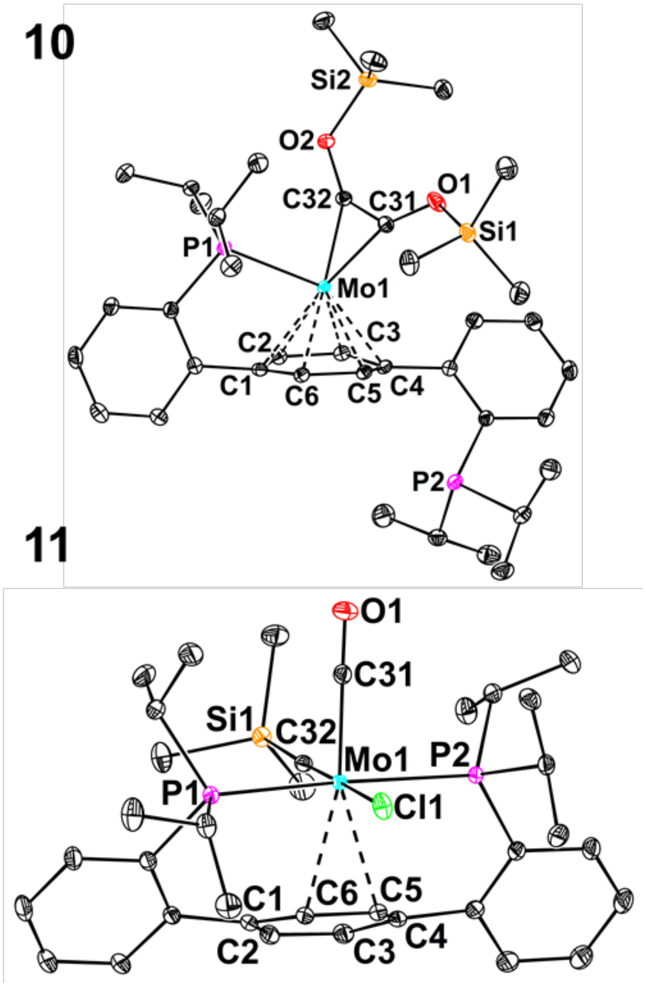

Figure 2: Solid-state structures of **10** and **11** with anisotropic displacement ellipsoids shown at the 50% probability level. Hydrogen atoms are omitted for clarity. Selected bond lengths [Å] and angles [°]: **10** Mo$_1$–C$_{arene}$(ave.) 2.280(2), Mo$_1$–C$_{31}$ 2.054(1), Mo$_1$–C$_{32}$ 2.032(1), C$_1$–C$_2$ 1.424(2), C$_2$–C$_3$ 1.427(2), C$_3$–C$_4$ 1.430(2), C$_4$–C$_5$ 1.430(2), C$_5$–C$_6$ 1.426(2), C$_6$–C$_1$ 1.428(2), C$_{31}$–O$_1$ 1.362(2), C$_{32}$–O$_2$ 1.368(2), C$_{31}$–C$_{32}$ 1.332(2), ∠ C$_{31}$-Mo$_1$-C$_{32}$ 38.02(6); **11** Mo$_1$–C$_5$ 2.524(1), Mo$_1$–C$_6$ 2.520(1), Mo$_1$–C$_{31}$ 1.976(1), Mo$_1$–C$_{32}$ 1.796(1), Mo$_1$–Cl$_1$ 2.588(1), C$_1$–C$_2$ 1.383(1), C$_2$–C$_3$ 1.407(1), C$_3$–C$_4$ 1.382(1), C$_4$–C$_5$ 1.421 (1), C$_5$–C$_6$ 1.395 (1), C$_6$–C$_1$ 1.424(1), C$_{31}$–O$_1$ 1.158(1), C$_{32}$–Si$_1$ 1.882(1).

C–O bond cleavage was observed, however, when a THF solution of dicarbyne **9-^{13}C** was warmed from -78 to 0 °C (Scheme 3). A broad resonance in the ^{31}P{^{1}H} NMR spectrum at 41.9 ppm supported the formation of a more oxidized Mo center. Signals in the $^{13}C\{^{1}H\}$ NMR spectrum at 344.9 and 241.9 ppm are consistent with silyl carbyne and carbonyl ligands, respectively. Mo(IV) trialkyl- and triaryl silyl carbyne complexes have been prepared previously and show diagnostic low-field ^{13}C NMR resonances in the range of 320-360 ppm.[70-72] Low temperature crystallization (-35 °C) provided single-crystals suitable for solid-state analysis, confirming this intermediate **11** as a constitutional isomer of the previously reported silyl carbyne **8** (Figure 2).[46] Contrasting the *pseudo*-square pyramidal geometry of carbyne **8**, isomer **11** adopts a *pseudo*-octahedral geometry with a clear η^2 metal-arene interaction; the $Mo{-}C_{arene}$ contacts average 2.52 Å in **11** compared to 2.82 Å in **8**. The $Mo\text{-}C_{32}$ distances are similar between the alkylidyne isomers (1.796(1) Å for **11**, 1.767(2) Å for **8**), with both being consistent with Mo−C triple bonds.[70,71,73,74]

Warming samples of silyl alkylidyne **11** resulted in isomerization within one hour to **8** at 25 °C as judged by $^{31}P\{^{1}H\}$ NMR spectroscopy (Figure S5). These data suggest that **11** is the kinetic product of carbide silylation. The *cis* geometry of the silyl carbyne moiety versus the central arene supports the proposed *pseudo*-square pyramidal geometry for carbide **7**, which forms immediately following C−O bond cleavage (Scheme 3). From **7**, electrophilic attack by silyl electrophile on the carbide followed by chloride coordination on the back-side of the molecule (as drawn) provides **11**. Although isomerization form **11** to **8** could occur in the six-coordinate complex by twists of trigonal faces of the octahedron, the rigidity of the terphenyl framework makes this mechanism unlikely.[75,76] It is proposed that dissociation of a ligand (chloride or phosphine) facilitates rearrangement to the thermodynamic product **8**, where the alkylidyne is now located *trans* to the arene ring, a sterically preferred coordination geometry (Table S2).

2.3. Mechanistic Investigation of C−O Bond Cleavage. From dicarbyne **9**, there are several envisioned pathways by which C−O bond cleavage could provide carbide **7** and hexamethyldisiloxane (Scheme 4, Paths 1-5). This reaction proceeds to completion in the course of *ca.* 2 h at 0 °C, to provide a mixture of **11** and **8**, without the spectroscopic observation of additional intermediates. If C−O bond cleavage proceeds from **9**, upon its formation in an irreversible process, three pathways are envisioned (Scheme 4, I). Intramolecular silyl ether formation—nucleophilic attack of a siloxide oxygen on the silyl group of the other siloxycarbyne ligand—would provide carbide **7** directly (Scheme 4, Path 1). Alternatively, external silyl electrophile attack on the siloxy carbyne oxygen could induce C−O bond cleavage to form a presumably highly unstable carbide/carbene complex, **B** (Scheme 4, Path 2). Silyl chloride elimination from this species would yield carbide **7**; subsequent

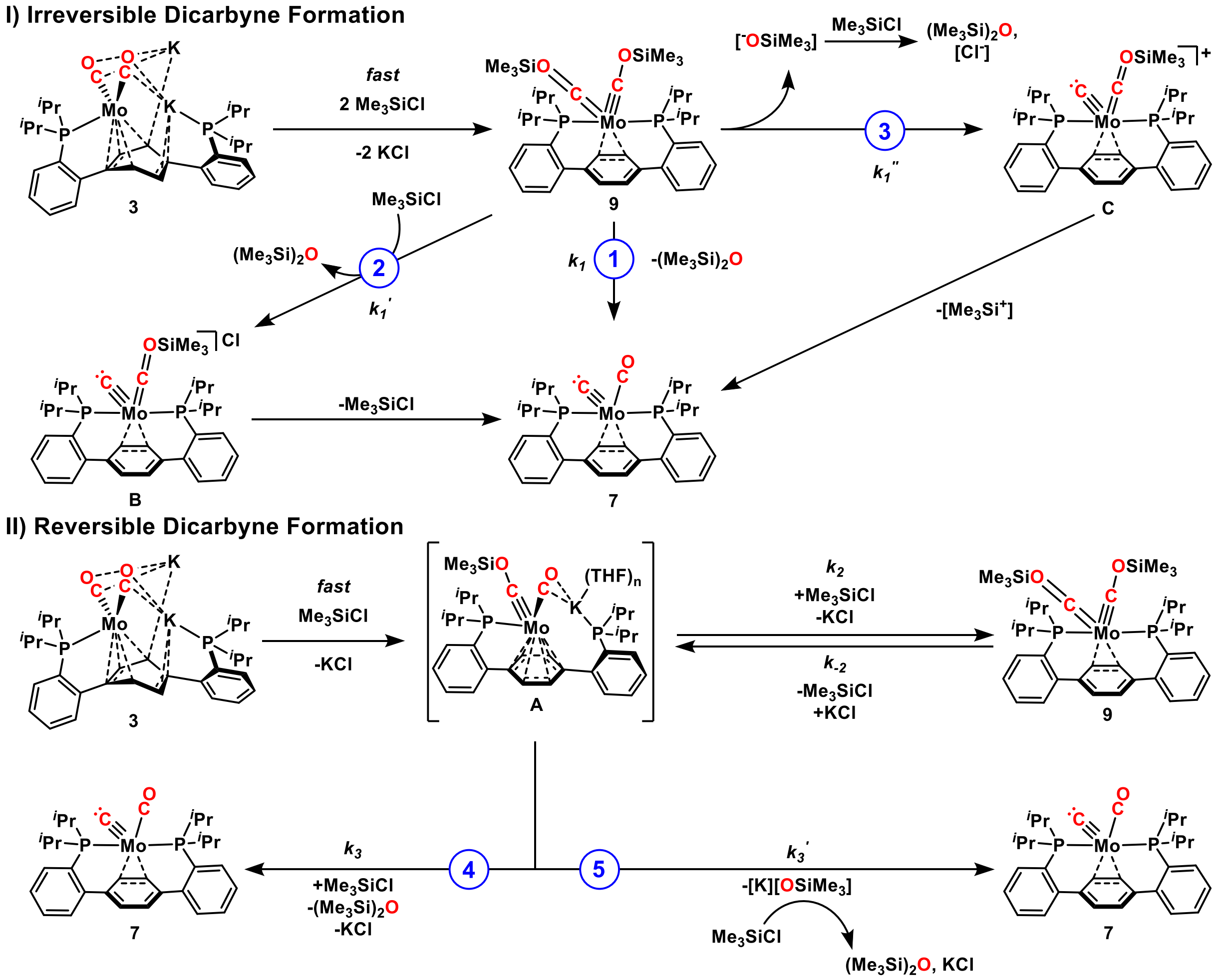

Scheme 4: Mechanistic possibilities (Paths 1-5, in blue) for the elementary reaction step of C−O bond cleavage from dicarbyne **9**.

silyl migration and chloride association would provide silyl alkylidyne **11**. C–O bond cleavage could also proceed from dicarbyne **9** via siloxide anion (Me_3SiO^-) dissociation, generating a cationic siloxycarbyne/carbide intermediate, **C** (Scheme 4, Path 3). This species could react with the released Me_3SiO^- to generate $(Me_3Si)_2O$, or lose Me_3Si^+ (or Me_3SiCl upon attack by Cl^-—under the reaction conditions, chloride anions are necessarily present in solution) which would undergo metal-free reaction with Me_3SiO^- to generate the observed $(Me_3Si)_2O$.

Both kinetics and isotopic labeling were employed to aid in experimentally evaluating these mechanistic possibilities. Kinetic analysis of the consumption of dicarbyne **9-^{13}C** and formation of silyl carbynes **11-^{13}C** and **8-^{13}C** at 0 °C (as at this temperature, carbide **7-^{13}C** is silylated rapidly (*vide infra*)) shows that the rate of C–O bond cleavage is independent of electrophile concentration (Figures 3 and S8). A zeroth order reaction in Me_3SiCl is consistent with two of these mechanistic scenarios (Eq. S1-S3); Path 2 is expected to show first order rate dependence on silyl electrophile concentration. Isotopic labeling studies invalidate both Paths 1 and 2. Condensing two equiv. of Me_3SiCl-d_9 onto a frozen THF solution of dianion **3-^{13}C** and allowing the mixture to thaw to -78 °C generated deuterated **9-^{13}C-*d*$_{18}$**. This dicarbyne complex was warmed to room temperature in the presence of an excess of $(CH_3)_3SiCl$, facilitating C–O bond cleavage, and the end products were analyzed by both NMR spectroscopy and GC/MS. The major hexamethyldisiloxane (HMDSO) isotopolog observed was HMDSO-d_{18} (81%, Scheme 5). Incorporation of at least one $(CH_3)_3Si$ group (as was observed in 19% of the product disiloxanes) excludes an intramolecular cleavage event (Scheme 4, I, Path 1). Electrophilic attack by external silyl electrophile, as in Path 2, can likewise be ruled out; if operative, this pathway would provide exclusively HMDSO-d_9. These results are further supported by the complementary experiment of warming **9-^{13}C** in an excess of $(CD_3)_3SiCl$ (Scheme 5).

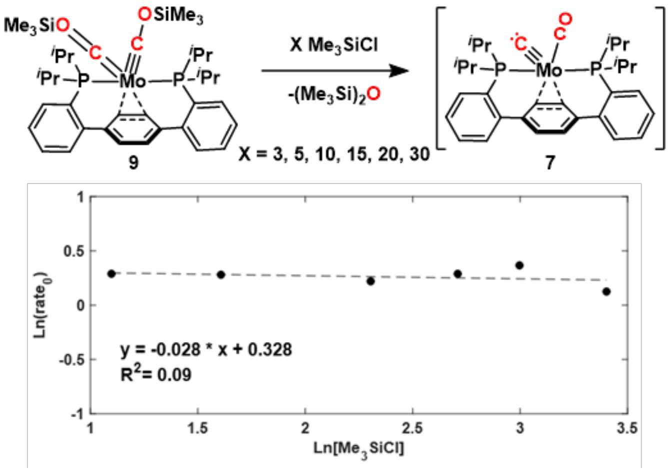

Figure 3: Kinetic data supporting C–O bond cleavage is zeroth order in silyl electrophile.

A siloxide dissociation pathway (Scheme 4, I, Path 3) is both zeroth order in silyl electrophile (Eq. S3) and accounts for the generation of all three HMDSO isotopologs. From **9-^{13}C-*d*$_{18}$**, the liberated siloxide anion could react with the proximal silyl group of cation **C** (giving HMDSO-d_{18}) or it could react off-metal with the excess Me_3SiCl (giving HMDSO-d_9). The preference for HMDSO-d_{18} is potentially a consequence of the high local concentration of **C**, which is expected to be a strong silylating agent. The formation of HMDSO-d_0, albeit in a small amount, is more convoluted as it requires a silyl group exchange. A control reaction demonstrates that Me_3SiO^- undergoes substitution chemistry with disiloxane, even in the presence of excess silyl electrophile (Figure S15). Such a side reaction accounts for the formation of the observed HMDSO-d_0 from the deutero dicarbyne. Assuming dicarbyne formation is irreversible, this pathway is the most consistent with both the reaction kinetics and labeling studies and cannot be ruled out based on the experimental data.

However, formation of dicarbyne **9** need not be irreversible (Scheme 4, II). Either a fast pre-equilibrium or rate limiting trimethylsilyl dissociation may precede C–O bond cleavage, via carbyne anion **A**. Anionic carbyne **A** can be envisioned to act as a precursor to C–O bond cleavage; electrophilic attack by external silyl chloride (Scheme 4, II, Path 4) or siloxide dissociation (Scheme 4, II, Path 5) would both result in direct generation of carbide **7**.

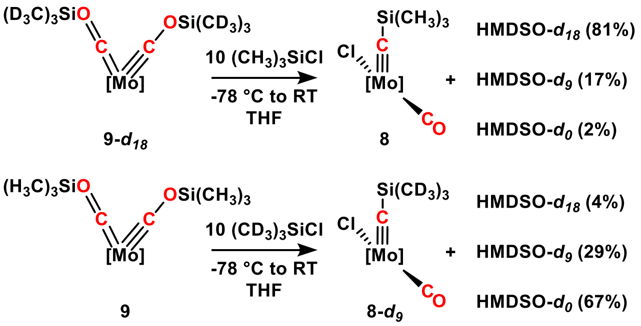

Scheme 5: End-product distributions in isotopic labeling studies of the C–O bond cleavage step. The *para*-terphenyldiphosphine ligand is omitted for brevity. Endproduct isotopolog distributions were determined by GC/MS.

Although a fast pre-equilibrium followed by reaction of **A** with external Me_3SiCl (Scheme 4, II, Path 5) would be overall zeroth order in electrophile (Eq. S4a), such a process can be ruled out by the isotopic labeling studies. Any pathway involving a fast pre-equilibrium would scramble the silyl electrophile label statistically, which is not observed either spectroscopically during the course of the reaction (^{2}H NMR, Figure S13) or in the end product isotopolog distributions (Scheme 5). Rate-limiting formation of **A** is likewise consistent with the observed reaction kinetics (Eqs. S6 and S7a). Further information was sought through direct studies of species **A**. Species **A** can be generated at low temperatures as part of a mixture, when using limiting amounts of electrophile. Careful addition of a single equiv. of Me_3SiCl to dianion **3-^{13}C** at -78 °C provides a mixture of **3-^{13}C**, dicarbyne **9-^{13}C**, and a third species. This new species displays $^{13}C\{^1H\}$ NMR resonances at 263.6 and 232.8 ppm, chemical shifts consistent with siloxycarbyne and carbonyl ligands, respectively. The $^{31}P\{^1H\}$ NMR spectrum shows signals at 97.7 and –2.8 ppm, supporting the tentative assignment of this new species as anionic carbyne **A** (Figure S16). Addition of a second equiv. of silyl electrophile to this mixture yields dicarbyne **9-^{13}C** almost quantitatively, consistent with **A** being a partially silylated species. Warming a mixture of **3-^{13}C**, **A**, and **9-^{13}C** to -50 °C demonstrates complete consumption of complex **A** by $^{13}C\{^1H\}$ and $^{31}P\{^1H\}$ NMR spectroscopies, the characteristic resonances of **3-^{13}C** and **9-^{13}C** persist at these temperatures. Anionic carbyne/CO adduct **A** forms a mixture of C–O cleaved products (Figure S17), as indicated by the characteristic low-field $^{13}C\{^1H\}$

NMR signals for silyl carbynes **8** and **11**, as well as mixed dicarbyne **15** (*vide infra*), observed upon exhaustively silylating this reaction mixture at -78 °C. These data are consistent with C–O bond cleavage occurring more readily from anionic carbyne **A** than neutral dicarbyne **9**, though C–O scission occurring from both complexes at 0 °C cannot be ruled out conclusively.

Though the end-product isotopolog distribution in a rate limiting silyl dissociation mechanism is convoluted by a dependence on the relative rates of C–O bond cleavage from **A** and resilylation of **A** to provide isotopologs of **9**, *in situ* ^{2}H NMR spectroscopy is more consistent with C–O scission by siloxide dissociation (Path 5) than external electrophile attack (Path 4). From **9**, no ^{2}H incorporation is observed in the metal complex during the course of the reaction with $(CD_3)_3SiCl$ (Figure S13), consistent with C–O bond cleavage being faster than resilylation at 0 °C. If formation of carbide **7** proceeded from **A** via external silyl electrophile attack (Path 4), HMDSO-d_9 would be formed starting from either **9** or **9-d_{18}**, inconsistent with the experimental data (Scheme 5). Moreover, this reactivity pathway fails to account for the HMDSO-d_0 and HMDSO-d_{18} observed from **9-d_{18}** and **9**, respectively. A siloxide dissociation pathway (Scheme 4, Path 5) is most consistent with the observed end-products, with off-metal substitution chemistry facilitating the formation of all three HMDSO isotopologs.

We therefore favor Path 5, a reaction mechanism in which silyl dissociation from dicarbyne **9** is rate limiting, providing anionic carbyne **A**, the precursor to C–O cleavage. At 0 °C, siloxide dissociates from this electron-rich species more rapidly than resilylation can occur—consistent with both spectroscopic studies and the observed reaction kinetics—providing carbide **7** and siloxide anion. As indicated above, direct siloxide dissociation from **9** (Path 3) is also a viable mechanism for carbide formation. The observation of C–O bond cleavage at lower temperature when starting from **A** is notable, and offers a method to facilitate selective deoxygenation chemistry, avoiding non-deoxygenative C–C coupling, by limiting electrophile concentration. These studies provide detailed mechanistic insight for an unprecedented observation of the elementary reaction step(s) of C–O bond cleavage to form a terminal transition metal carbide.

2.4. Reactions from Terminal Carbide 7. **7-^{13}C** is a spectroscopically observed intermediate in the addition of ^{i}Pr$_3$SiCl to dianion **3-^{13}C** *en route* to **5** and **6a** (Scheme 2). It is a proposed intermediate in the formation of trimethylsilyl alkylidyne **11** from dicarbyne **9** (Scheme 3). The addition of both electrophiles to independently prepared **7-^{13}C** was investigated at low temperature.

Treating a frozen THF solution of carbide **7-^{13}C** with one equiv. of Me$_3$SiCl resulted, upon warming to -78 °C, in complete disappearance of the carbidic resonance at 546.3 ppm and the growth in of the upfield shifted silylcarbyne resonances of **11-^{13}C** (*ca.* 75% by ^{31}P{^{1}H} NMR integration) and **8-^{13}C** (*ca.* 25% by ^{31}P{^{1}H} NMR integration) at 344.9 and 355.9 ppm, respectively (Scheme 6). These data support the hypothesis that **7-^{13}C** is a precursor to silyl alkylidynes **11** and **8** (*vide supra*). In contrast, addition of ^{i}Pr$_3$SiCl to a frozen THF solution of carbide **7-^{13}C** did not show any conversion of starting material upon thawing to -78 °C. The spectroscopic features of **7-^{13}C** persist in the ^{13}C{^{1}H} NMR spectrum up to -10 °C, at which temperature slow conversion to the triisopropylsilyl alkylidyne complex **12-^{13}C** (Scheme 6), is observed. Consistent with formation of this silyl carbyne are the upfield shifted resonance at 34.4 ppm in the ^{31}P{^{1}H} NMR spectrum, and resonances at 360.8 and 250.8 ppm in the ^{13}C{^{1}H} NMR spectrum. The stability of the carbide up to -10 °C in the presence of this bulky silyl electrophile is consistent with its spectroscopic detection in reactions of dianion **3-^{13}C** with ^{i}Pr$_3$SiCl (Scheme 2). However, formation of organic **6a** proceeds below this temperature when treating either anions **3** or **4** with ^{i}Pr$_3$SiCl, ruling out the intermediacy of isopropyl analogs of **8** and **11** at low temperatures. Based on this reactivity, coupling may occur from carbide **7-^{13}C** directly, which prompted investigation of reduction prior to silylation.

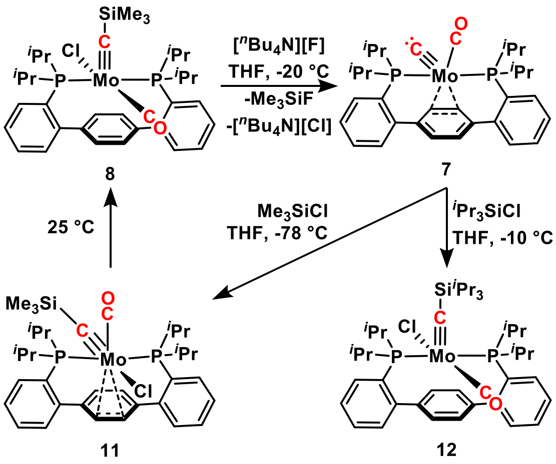

Scheme 6: *In situ* generation and silylation of terminal carbide **7**.

2.5. Investigation of C–C Bond Formation. Reduction of carbide **7** in the presence of silyl electrophiles was targeted. One equiv. of ^{i}Pr$_3$SiCl was added to *in situ* generated carbide **7-^{13}C** at -78 °C, resulting in no change to the ^{13}C{^{1}H} or ^{31}P{^{1}H} NMR spectra (Figure S19). Two equiv. of [Na][C$_{10}$H$_8$], as a solution in THF, were then added at low temperature. The ^{13}C{^{1}H} and ^{31}P{^{1}H} NMR spectra showed new broad resonances at 327.8 and 58.2 ppm, respectively. Expecting two resonances for the isotopically enriched nuclei in the ^{13}C NMR spectrum (given the chemically inequivalent C–Si and C–O motifs), the sample was cooled to -100 °C, resulting in further broadening, but maintenance of a single signal. Warming the sample to -60 °C resolved two broad ^{13}C resonances at 327.9 and 327.0 ppm, again in the chemical shift range of Mo alkylidynes. The product of carbide reduction in the presence of ^{i}Pr$_3$SiCl was tentatively assigned as silyl carbyne/oxycarbyne **13-^{13}C** (Scheme 7).

Independent synthesis of the trimethylsilyl variant (**14**) was targeted via reduction of silyl carbyne **8-^{13}C** (Scheme 7). Treatment with two equiv. of [Na][C$_{10}$H$_8$] at -78 °C demonstrated formation of a new species with broad resonances at 330.8 and 58.5 ppm in the ^{13}C{^{1}H} and ^{31}P{^{1}H} NMR spectra, respectively. The chemical shift differences between these resonances and those assigned to **13-^{13}C** are small, supporting assignment as the mixed carbyne **14-^{13}C** (Scheme 7). Cooling the sample to -100 °C resolved two broad triplets in the ^{13}C{^{1}H} NMR—that with the larger ^{2}J(C,P) (19.3 Hz) being shifted further downfield. Warming the sample to -60 °C likewise showed two resonances, now with the peak displaying the larger ^{2}J(C,P) (21.4 Hz) moving further upfield (Figure S20). The lack of C–C coupling in the ^{13}C{^{1}H} NMR spectrum supports the dicarbyne motif, and rules out silylated oxyacetylide or ketenylidene structures. Additional analysis of the temperature dependent fluxionality was inhibited by the narrow temperature range at which the complex is stable.

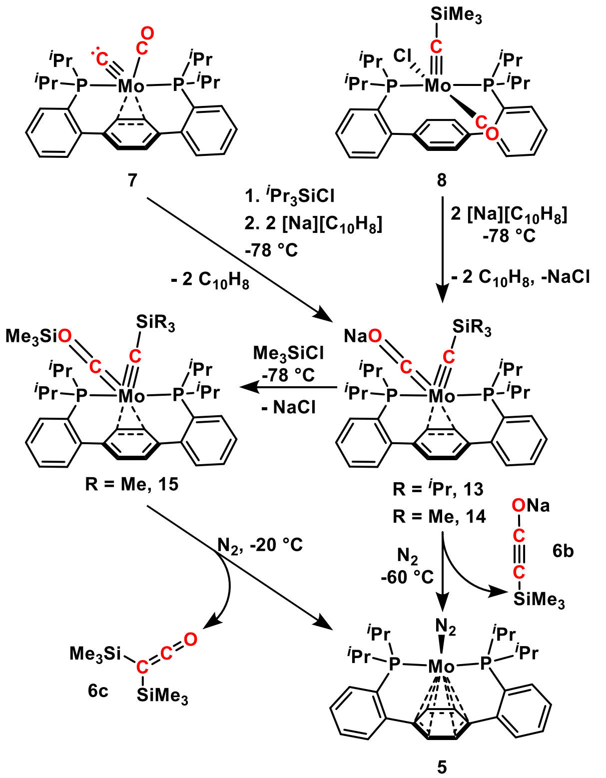

Scheme 7: Synthesis of mixed dicarbyne complexes and subsequent C–C bond formation.

Warming either **13**-^{13}**C** or **14**-^{13}**C** above -60 °C under N$_2$ resulted in conversion of the Mo species to dinitrogen complex **5**, and the growth in of a pair of doublets in the ^{13}C{^{1}H} NMR spectrum—131.3 and 5.9 ppm, ^1J(C,C) = 139.6 Hz—consistent with formation of sodium silyl ethynolate, **6b** (Scheme 6).[77] As reported previously,[78,79] addition of a small silyl electrophile to the trimethylsilyl ethynolate yielded disilyl ketene, **6c** (^{13}C{^{1}H} δ = 167.5 and 1.1 ppm, ^1J(C,C) = 82.3 Hz), the thermodynamically preferred isomer of the disilylated C$_2$O$_1$ product.

To gain further support for the proposed structures of anions **13**-^{13}**C** and **14**-^{13}**C**, silylation of the oxycarbyne fragment of **14**-^{13}**C** was attempted at low temperature, targeting a mixed silyl/siloxy dicarbyne, **15**-^{13}**C** (Scheme 7). Treating a solution of **14**-^{13}**C** with Me$_3$SiCl at -78 °C resulted in two new resonances in the ^{13}C{^{1}H} NMR spectrum at 378.9 and 283.7 ppm, assigned to the silyl- and siloxycarbyne resonances of **15**-^{13}**C**, respectively. The ^{31}P{^{1}H} NMR spectrum of **15**-^{13}**C** displays a broad apparent triplet at 56.8 ppm at -80 °C, lacking resolution necessary to assign two ^2J(P,C) coupling constants. Warming the sample to -20 °C resulted in resolution of this ^{31}P resonance to a doublet of doublets—^2J(P,C) = 18.3 and 13.4 Hz—consistent with the proposed mixed dicarbyne structure of **15**-^{13}**C**. The ^{13}C{^{1}H} NMR signals likewise were resolved as triplets, coupling the *trans*-spanning ^{31}P nuclei. Upon warming further, growth of dinitrogen complex **5** was observed as a singlet at 76.4 ppm in ^{31}P NMR spectrum. Concurrently, resonances in the ^{13}C{^{1}H} NMR showed formation of metal-free bis(trimethylsilyl)ketene **6c**.

Crossover experiments were performed to determine if the C–C bond forming step is unimolecular, both starting from silyl carbyne **8** and from a one-pot reduction and silylation of dicarbonyl dication **1** (Scheme 8). A 1:1 mixture of **8** and **8**-^{13}**C** was exposed to the conditions leading to C–C bond formation (Scheme 8). The organic fragment was interrogated by ^{13}C NMR spectroscopy for the presence of **6b** with a single ^{13}C enriched position. Only **6b**-^{13}**C** (displaying two ^{13}C enriched positions) is observed, consistent with intramolecular C–C bond formation. Formation of silyl ethynolates directly from mixed dicarbynes **13** and **14** indicates that the C–C bond is formed via reductive elimination of two cofacial carbyne ligands. Similarly, in the one-pot reduction and silylation of a mixture of **1** and **1**-^{13}**C**, only **6a**-^{13}**C** is observed.

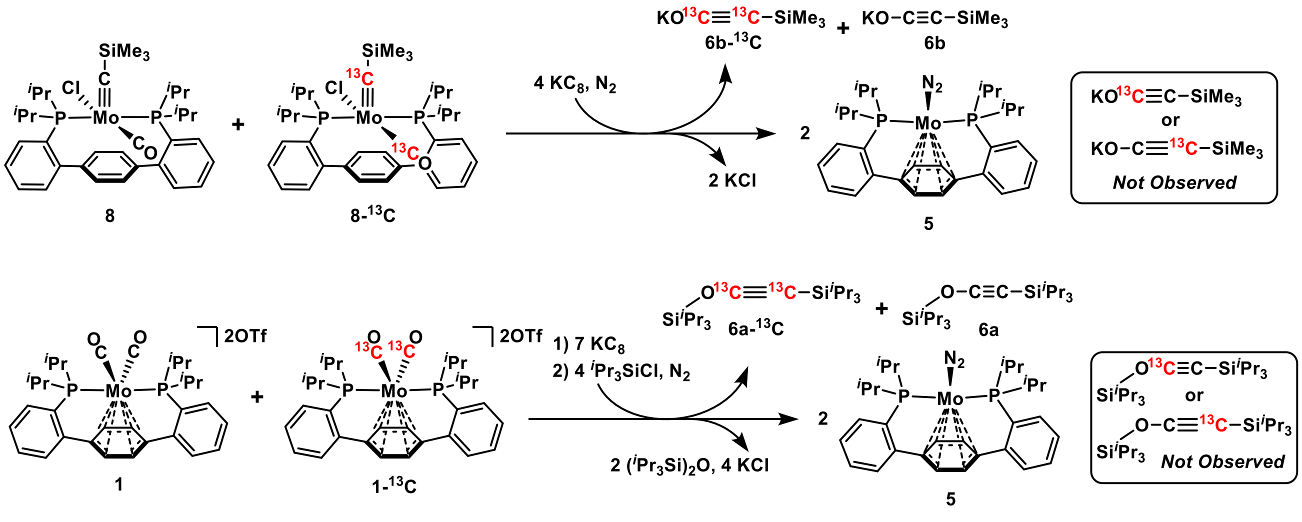

Scheme 8: Crossover-type experiments from **8**/**8**-^{13}**C** and **1**/**1**-^{13}**C**.

Though coupling of carbyne and CO ligands to form substituted oxyacetylenes is known,[50,80] these reactions involve electrophile addition at oxygen after C–C bond formation with ketenyl complexes as established reaction intermediates.[49,80,81] In contrast, complexes **13**-**15** demonstrate that in the present system, C–C bond formation occurs following functionalization at oxygen.

2.6. Quantum Mechanics Studies. With myriad complexes bearing Mo–C multiple bonds in a variety of coordination environments, calculations were performed to investigate the electronic structures of these molecules. Revised TPSS exchange and correlation functionals[82,83] were employed at the LANL2DZ[84-87] level of theory. The diisopropylphosphine and trimethylsilyl moieties were modeled as dimethylphosphine and silyl groups, respectively, unless noted otherwise. The optimized geometries of the computed structures agree well with experimentally determined solid-state parameters established by single-crystal XRD (for **2**, **8**, **10**, and **11**, Table S4). To further test the validity of the calculated structures, CO stretching frequencies and ^{13}C NMR shifts (GIAO)[88,89] were computed. The trends observed experimentally are matched well computationally (Table S3).

As a rare example of a terminal transition metal carbide,[44,45,90-95] the electronic structure of **7** is of particular interest. The highest occupied molecular orbital (HOMO) is non-bonding with respect to the carbide ligand and has stabilizing contributions from the π-acidic antibonding orbitals of both the central arene and the CO (Figure 4, a). The η^2 metal-arene interaction is supported experimentally; the arene ^{1}H and ^{13}C resonances of the metal-bound arene fragment show a distinct upfield shift (6.5 and 86.2 ppm, respectively), evidencing donation of electron density from Mo into an arene π* orbital. The Mo-carbide π-bonds show contributions from the metal d_{xz} and d_{yz} orbitals and C p_x and p_y orbitals (Figure 4, a, HOMO-2 and HOMO-3). The Mo-carbide σ-bond is slightly higher in energy (HOMO-1) with primarily C p_z character and contribution from a metal-based orbital of d_{z2} parentage (Figure S48). These results, in conjunction with natural population analysis, support a strong formal Mo≡C triple bond and agree well with computations for neutral Ru and Fe carbide complexes.[96,97]

The electronic structure of transition metal dicarbyne complexes has been studied extensively in the context of CO coupling.[98-100] The optimized structure of dicarbyne **9** shows short Mo–C distances of 1.850 Å, consistent with the proposed dicarbyne assignment. The Mo–C distance to the nearest arene carbons averages 2.593 Å, in agreement with the weak M-arene interaction inferred in solution from ^{1}H and ^{13}C{^{1}H} NMR spectroscopies. The four highest energy occupied molecular orbitals of **9** are composed of Mo d and C–O π* orbitals (Figure 4, b). Four orbitals have π contributions to the Mo–C bonds, in two orthogonal pairs. The HOMO-1 and HOMO-2, with metal orbital contributions of d_{xz} and d_{yz} parentage (Figure S51), show considerable in-phase orbital overlap between the carbyne carbons, akin to calculations performed for adjacent cylindrical π-interacting ligands on the unique face of a capped trigonal prism.[98]

The frontier molecular orbitals of mixed dicarbyne **15** (Figure 4, c) are quite similar to **9** (Figure 4, b), again demonstrating significant in-phase orbital overlap between the carbyne C atoms. Contraction of the C–Mo–C angle, as would be expected in the reaction coordinate for formation of a C–C bond from either **9** or **15**, would stabilize these orbitals (for instance, they become the C–C π-bonds of the alkyne fragment in **10**, Figure 4, d), an electronic justification for the observed C–C bond formation from these intermediates.[99,101] All of these orbitals are comparable to those calculated for model systems for carbyne-carbyne coupling—a hypothetical tungsten dicarbyne[99,100] and an isolated iron diphosphine dicarbyne.[33]

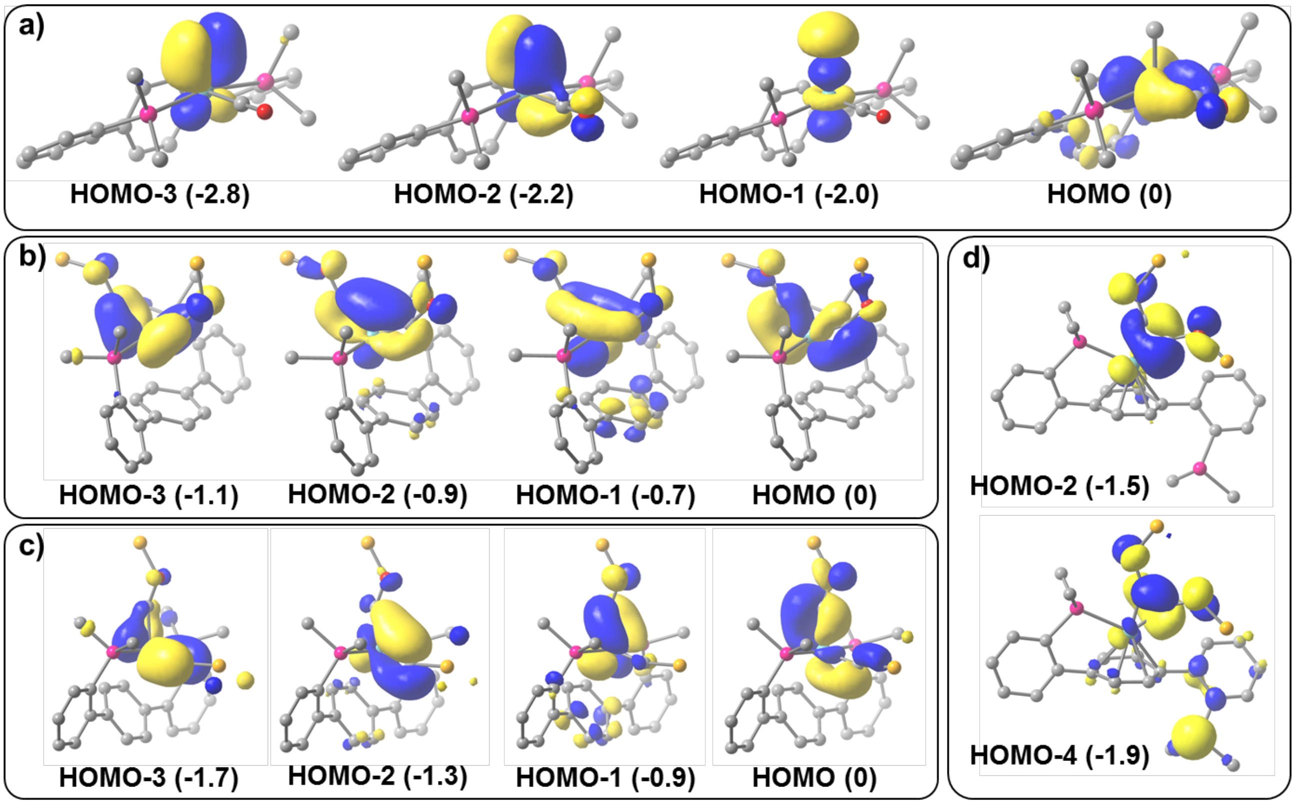

Figure 4: Calculated valence molecular orbitals of models of **7** (a), **9** (b), **15** (c), and **10** (d). Orbital energies (relative to the HOMO) in eV are given in parentheses. Isosurfaces are displayed at the 0.04 e/Å^3 level.

Conclusions

Crystallography, isotopic labeling, kinetics, spectroscopy, and computation have provided insight into the mechanism by which Mo-bound CO molecules can be cleaved and coupled to a C_2O_1 product at a single metal center supported by a terphenyl diphosphine ligand. When dianion **3** is treated with Me_3SiCl, a bis(siloxycarbyne) complex is formed, the first example of Mo supporting such a motif. This species can either undergo C–C coupling—forming a bis(siloxy)acetylene adduct of Mo, a two electron CO coupling product—or it can undergo C–O cleavage. Kinetics and isotopic labeling studies are consistent with two mechanisms, one involving rate determining siloxide dissociation, the second silyl electrophile dissociation followed by fast siloxide loss. An anionic Mo-siloxycarbyne/CO species indeed undergoes C–O cleavage at low temperatures and demonstrates that scission of this bond is more facile from a mono- rather than bis-silylated species.

The carbide resulting from C–O bond cleavage is trapped rapidly in the presence of excess electrophile at the temperatures required to break the C–O bond, giving a *pseudo*-octahedral silylalkylidyne complex. Further warming results in rearrangement to the thermodynamic product, a sterically preferred five-coordinate isomer lacking a metal-arene interaction. Reduction of this species at low temperature provides evidence for a mixed dicarbyne, which undergoes C–C bond formation at temperatures as low as -60 °C, releasing the silylethynolate fragment and binding dinitrogen to give the final product **5**.

Combined, the findings above provide valuable insight into the use of coordinatively flexible, redox noninnocent ligand scaffolds for multi-electron small molecule transformations. The adaptive binding of the arene plays a central role in the stabilization of unique molecular motifs throughout the reaction scheme—ranging from an extremely reducing trianion to high-valent molybdenum complexes bearing Mo–C multiple bonds: dicarbyne, carbide, and alkylidyne complexes. Phosphine arm hemilability is likewise critical for accessing the highly reduced species. Work to tune the selectivity and expand the scope of this reductive functionalization chemistry to other electrophiles and small molecule substrates is ongoing.

ASSOCIATED CONTENT

Supporting Information.

Detailed experimental procedures, full characterization, crystallographic details (CIF), and spectroscopic data. This material is available free of charge via the Internet at http://pubs.acs.org.

AUTHOR INFORMATION

Corresponding Author

*E-mail: agapie@caltech.edu

ACKNOWLEDGMENT

We thank Larry Henling and Mike Takase for invaluable crystallographic assistance and David VanderVelde for NMR expertise. We are grateful to Jay Labinger for insightful suggestions regarding the synthesis of mixed molybdenum dicarbyne complexes. Sibo Lin is thanked for advice and discussions regarding the computations. T.A. is grateful for Sloan and Dreyfus fellowships and J.A.B. for a NSF graduate research fellowship. This research was funded by the NSF (CHE-1151918) and Caltech.

REFERENCES

(1) Appel, A. M.; Bercaw, J. E.; Bocarsly, A. B.; Dobbek, H.; DuBois, D. L.; Dupuis, M.; Ferry, J. G.; Fujita, E.; Hille, R.; Kenis, P. J. A.; Kerfeld, C. A.; Morris, R. H.; Peden, C. H. F.; Portis, A. R.; Ragsdale, S. W.; Rauchfuss, T. B.; Reek, J. N. H.; Seefeldt, L. C.; Thauer, R. K.; Waldrop, G. L. *Chem. Rev.* **2013**, *113*, 6621.

(2) Wayland, B.; Fu, X. F. *Science* **2006**, *311*, 790.

(3) West, N. M.; Miller, A. J. M.; Labinger, J. A.; Bercaw, J. E. *Coord. Chem. Rev.* **2011**, *255*, 881.

(4) Rofer-DePoorter, C. K. *Chem. Rev.* **1981**, *81*, 447.

(5) Maitlis, P. M.; Zanotti, V. *Chem. Commun.* **2009**, 1619.

(6) Jiao, F.; Li, J.; Pan, X.; Xiao, J.; Li, H.; Ma, H.; Wei, M.; Pan, Y.; Zhou, Z.; Li, M.; Miao, S.; Li, J.; Zhu, Y.; Xiao, D.; He, T.; Yang, J.; Qi, F.; Fu, Q.; Bao, X. *Science* **2016**, *351*, 1065.

(7) Evans, W. J.; Grate, J. W.; Hughes, L. A.; Zhang, H.; Atwood, J. L. *J. Am. Chem. Soc.* **1985**, *107*, 3728.

(8) Evans, W. J.; Lee, D. S.; Ziller, J. W.; Kaltsoyannis, N. *J. Am. Chem. Soc.* **2006**, *128*, 14176.

(9) Summerscales, O. T.; Cloke, F. G. N.; Hitchcock, P. B.; Green, J. C.; Hazari, N. *Science* **2006**, *311*, 829.

(10) Summerscales, O. T.; Cloke, F. G. N.; Hitchcock, P. B.; Green, J. C.; Hazari, N. *J. Am. Chem. Soc.* **2006**, *128*, 9602.

(11) Frey, A. S.; Cloke, F. G. N.; Hitchcock, P. B.; Day, I. J.; Green, J. C.; Aitken, G. *J. Am. Chem. Soc.* **2008**, *130*, 13816.

(12) Frey, A. S. P.; Cloke, F. G. N.; Coles, M. P.; Maron, L.; Davin, T. *Angew. Chem. Int. Ed.* **2011**, *50*, 6881.

(13) Gardner, B. M.; Stewart, J. C.; Davis, A. L.; McMaster, J.; Lewis, W.; Blake, A. J.; Liddle, S. T. *Proc. Natl. Acad. Sci. U.S.A.* **2012**, *109*, 9265.

(14) Manriquez, J. M.; McAlister, D. R.; Sanner, R. D.; Bercaw, J. E. *J. Am. Chem. Soc.* **1976**, *98*, 6733.

(15) LaPointe, R. E.; Wolczanski, P. T.; Mitchell, J. F. *J. Am. Chem. Soc.* **1986**, *108*, 6382.

(16) Neithamer, D. R.; LaPointe, R. E.; Wheeler, R. A.; Richeson, D. S.; Van Duyne, G. D.; Wolczanski, P. T. *J. Am. Chem. Soc.* **1989**, *111*, 9056.

(17) Miller, R. L.; Wolczanski, P. T.; Rheingold, A. L. *J. Am. Chem. Soc.* **1993**, *115*, 10422.

(18) Miller, A. J. M.; Labinger, J. A.; Bercaw, J. E. *J. Am. Chem. Soc.* **2008**, *130*, 11874.

(19) Wolczanski, P. T.; Bercaw, J. E. *Acc. Chem. Res.* **1980**, *13*, 121.

(20) Belmonte, P. A.; Cloke, F. G. N.; Schrock, R. R. *J. Am. Chem. Soc.* **1983**, *105*, 2643.

(21) Watanabe, T.; Ishida, Y.; Matsuo, T.; Kawaguchi, H. *J. Am. Chem. Soc.* **2009**, *131*, 3474.

(22) Matsuo, T.; Kawaguchi, H. *J. Am. Chem. Soc.* **2005**, *127*, 17198.

(23) Okazaki, M.; Ohtani, T.; Inomata, S.; Tagaki, N.; Ogino, H. *J. Am. Chem. Soc.* **1998**, *120*, 9135.

(24) Shima, T.; Hou, Z. *J. Am. Chem. Soc.* **2006**, *128*, 8124.

(25) Matsuo, T.; Kawaguchi, H. *J. Am. Chem. Soc.* **2005**, *127*, 17198.

(26) Wayland, B. B.; Sherry, A. E.; Coffin, V. L. *J. Chem. Soc. Chem. Commun.* **1989**, 662.

(27) Sherry, A. E.; Wayland, B. B. *J. Am. Chem. Soc.* **1989**, *111*, 5010.

(28) Carnahan, E. M.; Protasiewicz, J. D.; Lippard, S. J. *Acc. Chem. Res.* **1993**, *26*, 90.

(29) Vrtis, R. N.; Rao, C. P.; Bott, S. G.; Lippard, S. J. *J. Am. Chem. Soc.* **1988**, *110*, 7564.

(30) Bianconi, P. A.; Williams, I. D.; Engeler, M. P.; Lippard, S. J. *J. Am. Chem. Soc.* **1986**, *108*, 311.

(31) Bennett, M. J.; Graham, W. A. G.; Smith, R. A.; Stewart, R. P. *J. Am. Chem. Soc.* **1973**, *95*, 1684.

(32) Protasiewicz, J. D.; Lippard, S. J. *J. Am. Chem. Soc.* **1991**, *113*, 6564.

(33) Suess, D. L. M.; Peters, J. C. *J. Am. Chem. Soc.* **2013**, *135*, 12580.

(34) Protasiewicz, J. D.; Masschelein, A.; Lippard, S. J. *J. Am. Chem. Soc.* **1993**, *115*, 808.

(35) Li, C. W.; Ciston, J.; Kanan, M. W. *Nature* **2014**, *508*, 504.

(36) Hu, Y. L.; Lee, C. C.; Ribbe, M. W. *Science* **2011**, *333*, 753.

(37) Lee, C. C.; Hu, Y. L.; Ribbe, M. W. *Science* **2010**, *329*, 642.

(38) Yang, Z. Y.; Dean, D. R.; Seefeldt, L. C. *J. Biol. Chem.* **2011**, *286*, 19417.

(39) Yan, L.; Dapper, C. H.; George, S. J.; Wang, H.; Mitra, D.; Dong, W.; Newton, W. E.; Cramer, S. P. *Eur. J. Inorg. Chem.* **2011**, *2011*, 2064.

(40) Spatzal, T.; Perez, K. A.; Einsle, O.; Howard, J. B.; Rees, D. C. *Science* **2014**, *345*, 1620.

(41) Dance, I. *Dalton Trans.* **2011**, *40*, 5516.
(42) Dance, I. *Chem. Commun.* **2013**, *49*, 10893.
(43) Horwitz, C. P.; Shriver, D. F. *J. Am. Chem. Soc.* **1985**, *107*, 8147.
(44) Peters, J. C.; Odom, A. L.; Cummins, C. C. *Chem. Commun.* **1997**, 1995.
(45) Enriquez, A. E.; White, P. S.; Templeton, J. L. *J. Am. Chem. Soc.* **2001**, *123*, 4992.
(46) Buss, J. A.; Agapie, T. *Nature* **2016**, *529*, 72.
(47) Shilov, A. E. *Russ. Chem. Bull.* **2003**, *52*, 2555.
(48) Churchill, M. R.; Wasserman, H. J.; Holmes, S. J.; Schrock, R. R. *Organometallics* **1982**, *1*, 766.
(49) Kreissl, F. R.; Frank, A.; Schubert, U.; Lindner, T. L.; Huttner, G. *Angew. Chem. Int. Ed.* **1976**, *15*, 632.
(50) Fischer, E. O.; Friedrich, P. *Angew. Chem. Int. Ed.* **1979**, *18*, 327.
(51) Mayr, A.; Hoffmeister, H. *Adv. Organomet. Chem.* **1991**, *32*, 227.
(52) Templeton, J. L. *Adv. Organomet. Chem.* **1989**, *29*, 1.
(53) Velian, A.; Lin, S.; Miller, A. J. M.; Day, M. W.; Agapie, T. *J. Am. Chem. Soc.* **2010**, *132*, 6296.
(54) Lin, S.; Day, M. W.; Agapie, T. *J. Am. Chem. Soc.* **2011**, *133*, 3828.
(55) Herbert, D. E.; Lara, N. C.; Agapie, T. *Chem. Eur. J.* **2013**, *19*, 16453.
(56) Horak, K. T.; Velian, A.; Day, M. W.; Agapie, T. *Chem. Commun.* **2014**, *50*, 4427.
(57) Henthorn, J. T.; Lin, S.; Agapie, T. *J. Am. Chem. Soc.* **2015**, *137*, 1458.
(58) Horak, K. T.; Agapie, T. *J. Am. Chem. Soc.* **2016**, *138*, 3443.
(59) Buss, J. A.; Edouard, G. A.; Cheng, C.; Shi, J.; Agapie, T. *J. Am. Chem. Soc.* **2014**, *136*, 11272.
(60) Cassani, M. C.; Gun'ko, Y. K.; Hitchcock, P. B.; Lappert, M. F.; Laschi, F. *Organometallics* **1999**, *18*, 5539.
(61) Sattler, A.; Parkin, G. *J. Am. Chem. Soc.* **2012**, *134*, 2355.
(62) Dougherty, D. A. *Science* **1996**, *271*, 163.
(63) D-block transition metals lack the requisite d orbitals to form four independent π-bonds; however, we employ the "bis-carbyne" nomenclature rather than "bis-carbene" or "carbene-carbyne" in accord with the single substituent at carbon. This nomenclature conforms to IUPAC conventions: McNaught, A. D.; Wilkinson, A. *IUPAC Compendium of Chemical Terminology*, 2nd ed.; Blackwell Scientific Publications: Oxford, 1997. Structural representations of these complexes are drawn with arbitrarily assigned $M{\equiv}CR$ and $M{=}CR$ bonds to reflect the electronic structure limitation of three total π-bonds.
(64) Lee, Y.; Peters, J. C. *J. Am. Chem. Soc.* **2011**, *133*, 4438.
(65) Vrtis, R. N.; Liu, S.; Rao, C. P.; Bott, S. G.; Lippard, S. J. *Organometallics* **1991**, *10*, 275.
(66) Filippou, A. C.; Hofmann, P.; Kiprof, P.; Schmid, H. R.; Wagner, C. *J. Organomet. Chem.* **1993**, *459*, 233.
(67) Filippou, A. C.; Völkl, C.; Grünleitner, W.; Kiprof, P. *J. Organomet. Chem.* **1992**, *434*, 201.
(68) Wang, Y.; Da Silva, J. J. R. F.; Pombeiro, A. J. L.; Pellinghelli, M. A.; Tiripicchio, A.; Henderson, R. A.; Richards, R. L. *J. Chem. Soc., Dalton Trans.* **1995**, 1183.
(69) Filippou, A. C.; Grünleitner, W.; Völkl, C.; Kiprof, P. Fischer, E. O.; Friedrich, P. *Angew. Chem. Int. Ed.* **1991**, *30*, 1167.
(70) Ahmed, K. J.; Chisholm, M. H.; Huffman, J. C. *Organometallics* **1985**, *4*, 1168.
(71) Cordiner, R. L.; Hill, A. F.; Shang, R.; Willis, A. C. *Organometallics* **2011**, *30*, 139.
(72) Jamison, G. M.; Bruce, A. E.; White, P. S.; Templeton, J. L. *J. Am. Chem. Soc.* **1991**, *113*, 5057.
(73) Cochran, F. V.; Schrock, R. R. *Organometallics* **2001**, *20*, 2127.
(74) Filippou, A. C.; Grünleitner, W.; Fischer, E. O.; Imhof, W.; Huttner, G. *J. Organomet. Chem.* **1991**, *413*, 165.
(75) Fay, R. C.; Lindmark, A. F. *J. Am. Chem. Soc.* **1983**, *105*, 2118.
(76) Marinescu, S. C.; Agapie, T.; Day, M. W.; Bercaw, J. E. *Organometallics* **2007**, *26*, 1178.
(77) Ito, M.; Shirakawa, E.; Takaya, H. *Synlett.* **2002**, 1329.
(78) Groh, B. L.; Magrum, G. R.; Barton, T. J. *J. Am. Chem. Soc.* **1987**, *109*, 7568.
(79) Nikolaeva, S. N.; Ponomarev, S. V.; Petrosyan, V. S.; Lorberth, J. *J. Organomet. Chem.* **1997**, *535*, 213.
(80) Kreissl, F. R.; Sieber, W.; Wolfgruber, M. *Angew. Chem. Int. Ed.* **1983**, *22*, 493.
(81) Kreissl, F. R.; Uedelhoven, W.; Eberl, K. *Angew. Chem. Int. Ed.* **1978**, *17*, 859.
(82) Perdew, J. P.; Ruzsinszky, A.; Csonka, G. I.; Constantin, L. A.; Sun, J. *Phys. Rev. Lett.* **2009**, *103*, 026403.
(83) Perdew, J. P.; Ruzsinszky, A.; Csonka, G. I.; Constantin, L. A.; Sun, J. *Phys. Rev. Lett.* **2011**, *106*, 179902.
(84) Dunning, T. H.; Hay, P. J. In *Methods of Electronic Structure Theory*; Schaefer, H. F., Ed.; Springer US: Boston, MA, 1977, p 1.
(85) Hay, P. J.; Wadt, W. R. *J. Chem. Phys.* **1985**, *82*, 270.
(86) Wadt, W. R.; Hay, P. J. *J. Chem. Phys.* **1985**, *82*, 284.
(87) Hay, P. J.; Wadt, W. R. *J. Chem. Phys.* **1985**, *82*, 299.
(88) Wolinski, K.; Hinton, J. F.; Pulay, P. *J. Am. Chem. Soc.* **1990**, *112*, 8251.
(89) Cheeseman, J. R.; Trucks, G. W.; Keith, T. A.; Frisch, M. J. *J. Chem. Phys.* **1996**, *104*, 5497.
(90) Greco, J. B.; Peters, J. C.; Baker, T. A.; Davis, W. M.; Cummins, C. C.; Wu, G. *J. Am. Chem. Soc.* **2001**, *123*, 5003.
(91) Hejl, A.; Trnka, T. M.; Day, M. W.; Grubbs, R. H. *Chem. Commun.* **2002**, 2524.
(92) Carlson, R. G.; Gile, M. A.; Heppert, J. A.; Mason, M. H.; Powell, D. R.; Velde, D. V.; Vilain, J. M. *J. Am. Chem. Soc.* **2002**, *124*, 1580.
(93) Romero, P. E.; Piers, W. E.; McDonald, R. *Angew. Chem. Int. Ed.* **2004**, *43*, 6161.
(94) Morsing, T. J.; Reinholdt, A.; Sauer, S. P. A.; Bendix, J. *Organometallics* **2016**, *35*, 100.
(95) Stewart, M. H.; Johnson, M. J. A.; Kampf, J. W. *Organometallics* **2007**, *26*, 5102.
(96) Gary, J. B.; Buda, C.; Johnson, M. J. A.; Dunietz, B. D. *Organometallics* **2008**, *27*, 814.
(97) Krapp, A.; Pandey, K. K.; Frenking, G. *J. Am. Chem. Soc.* **2007**, *129*, 7596.
(98) Hoffmann, R.; Beier, B. F.; Muetterties, E. L.; Rossi, A. R. *Inorg. Chem.* **1977**, *16*, 511.
(99) Hoffmann, R.; Wilker, C. N.; Lippard, S. J.; Templeton, J. L.; Bower, D. C. *J. Am. Chem. Soc.* **1983**, *105*, 146.
(100) Wilker, C. N.; Hoffmann, R.; Eisenstein, O. *Nouv. J. Chim.* **1983**, *7*, 535.
(101) Brower, D. C.; Templeton, J. L.; Mingos, D. M. P. *J. Am. Chem. Soc.* **1987**, *109*, 5203.

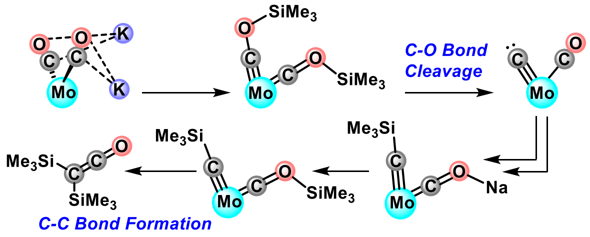
O
C
O
C
K
K
Mo
SiMe3
O
C
Mo
C
O
SiMe3
C-O Bond
Cleavage
C
C
O
Mo
Me3Si
C
Mo
C
O
Na
Me3Si
C
Mo
C
O
SiMe3
Me3Si
C
C
O
SiMe3
C-C Bond Formation